Provided for non-commercial research and education use.
Not for reproduction, distribution or commercial use.

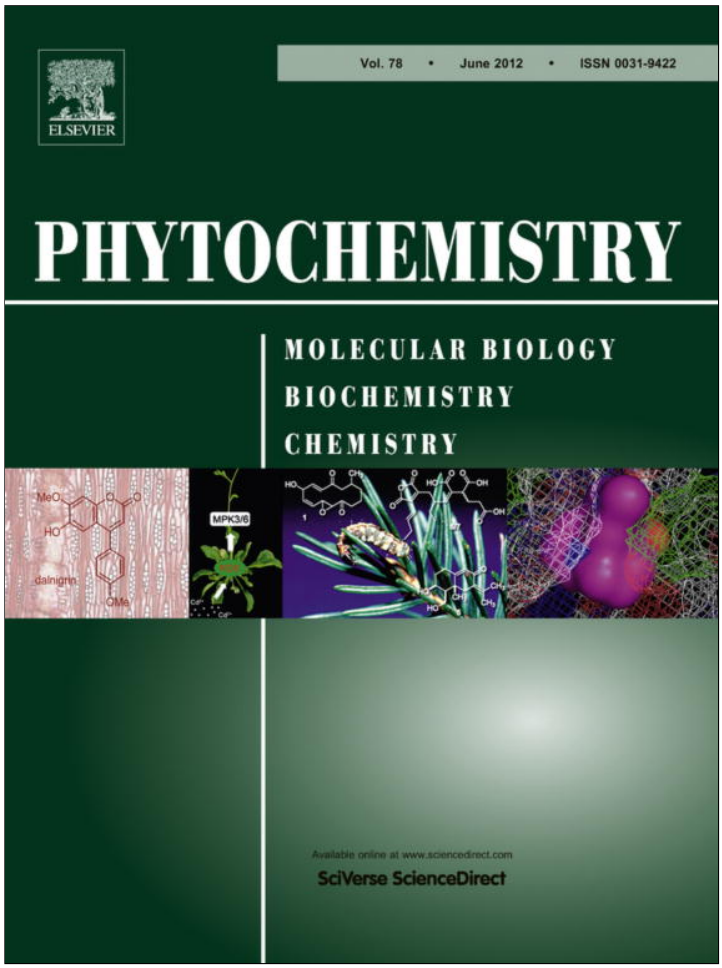

This article appeared in a journal published by Elsevier. The attached copy is furnished to the author for internal non-commercial research and education use, including for instruction at the authors institution and sharing with colleagues.

Other uses, including reproduction and distribution, or selling or licensing copies, or posting to personal, institutional or third party websites are prohibited.

In most cases authors are permitted to post their version of the article (e.g. in Word or Tex form) to their personal website or institutional repository. Authors requiring further information regarding Elsevier's archiving and manuscript policies are encouraged to visit:

http://www.elsevier.com/copyright

Author's personal copy

Phytochemistry 78 (2012) 135–146

Contents lists available at SciVerse ScienceDirect

Phytochemistry

journal homepage: www.elsevier.com/locate/phytochem

Distinct chemotypes of *Tephrosia vogelii* and implications for their use in pest control and soil enrichment

Philip C. Stevenson [a,b,*], Geoffrey C. Kite [b], Gwilym P. Lewis [b], Félix Forest [b], Stephen P. Nyirenda [c], Steven R. Belmain [a], Gudeta W. Sileshi [d], Nigel C. Veitch [b]

[a] Natural Resources Institute, University of Greenwich, Central Avenue, Chatham Maritime, Kent ME4 4TB, UK
[b] Royal Botanic Gardens, Kew, Richmond, Surrey TW9 3DS, UK
[c] Department of Agricultural Research Services, Lunyangwa Research Station, P.O. Box 59, Mzuzu, Malawi
[d] World Agroforestry Centre (ICRAF), Southern Africa Programme, Chitedze Agricultural Research Station, P.O. Box 30798, Lilongwe, Malawi

ARTICLE INFO

Article history:
Received 19 December 2011
Received in revised form 24 February 2012
Available online 4 April 2012

Keywords:
Tephrosia vogelii
Tephrosia candida
Leguminosae
Flavanones
Dihydroflavonol
Flavonol glycosides
Rotenoids
Pesticidal plants

ABSTRACT

Tephrosia vogelii Hook. f. (Leguminosae) is being promoted as a pest control and soil enrichment agent for poorly-resourced small-scale farmers in southern and eastern Africa. This study examined plants being cultivated by farmers and found two chemotypes. Chemotype 1 (C1) contained rotenoids, including deguelin, rotenone, sarcolobine, tephrosin and α-toxicarol, required for pest control efficacy. Rotenoids were absent from chemotype 2 (C2), which was characterised by prenylated flavanones, including the previously unrecorded examples (2*S*)-5,7-dimethoxy-8-(3-hydroxy-3-methylbut-1*Z*-enyl)flavanone, (2*S*)-5,7-dimethoxy-8-(3-methylbut-1,3-dienyl)flavanone, (2*S*)-4′-hydroxy-5-methoxy-6″,6″-dimethylpyrano[2″,3″:7,8]flavanone, (2*S*)-5-methoxy-6″,6″-dimethyl-4″,5″-dihydrocyclopropa[4″,5″]furano[2″,3″:7,8]flavanone, (2*S*)-7-hydroxy-5-methoxy-8-prenylflavanone, and (2*R*,3*R*)-3-hydroxy-5-methoxy-6″,6″-dimethylpyrano[2″,3″:7,8]flavanone. The known compounds (2*S*)-5-methoxy-6″,6″-dimethylpyrano[2″,3″:7,8]flavanone (obovatin 5-methyl ether) and 5,7-dimethoxy-8-(3-hydroxy-3-methylbut-1*Z*-enyl)flavone (*Z*-tephrostachin) were also found in C2. This chemotype, although designated *Tephrosia candida* DC. in collections originating from the World Agroforestry Centre (ICRAF), was confirmed to be *T. vogelii* on the basis of morphological comparison with verified herbarium specimens and DNA sequence analysis. Sampling from 13 locations in Malawi where farmers cultivate *Tephrosia* species for insecticidal use indicated that almost 1 in 4 plants were *T. vogelii* C2, and so were unsuitable for this application. Leaf material sourced from a herbarium specimen of *T. candida* contained most of the flavanones found in *T. vogelii* C2, but no rotenoids. However, the profile of flavonol glycosides was different to that of *T. vogelii* C1 and C2, with 6-hydroxykaempferol 6-methyl ether as the predominant aglycone rather than kaempferol and quercetin. The structures of four unrecorded flavonol glycosides present in *T. candida* were determined using cryoprobe NMR spectroscopy and MS as the 3-*O*-α-rhamnopyranosyl(1 → 6)-β-galactopyranoside-7-*O*-α-rhamnopyranoside, 3-*O*-α-rhamnopyranosyl(1 → 2)[α-rhamnopyranosyl(1 → 6)]-β-galactopyranoside, 3-*O*-α-rhamnopyranosyl-(1 → 2)[α-rhamnopyranosyl(1 → 6)]-β-galactopyranoside-7-*O*-α-rhamnopyranoside, and 3-*O*-α-rhamnopyranosyl (1 → 2)[(3-*O*-*E*-feruloyl)-α-rhamnopyranosyl(1 → 6)]-β-galactopyranosides of 6-hydroxykaempferol 6-methyl ether. Tentative structures for a further 37 flavonol glycosides of *T. candida* were assigned by LC–MS/MS. The correct chemotype of *T. vogelii* (*i.e.* C1) needs to be promoted for use by farmers in pest control applications.

© 2012 Elsevier Ltd. All rights reserved.

1. Introduction

Tephrosia Pers. (Leguminosae) is a large pantropical genus of more than 350 species, many of which have important traditional uses (Schrire, 2005). Among these, *Tephrosia vogelii* Hook. f. has been used widely across Africa as a fish poison, pesticide and for soil enrichment (Burkill, 1995; Kamanula et al., 2011; Mafongoya and Kuntashula, 2005; Neuwinger, 2004; Nyirenda et al., 2011; Sileshi et al., 2005; Sirrine et al., 2010). The pesticidal and insecticidal activities of *T. vogelii* are likely to be due to the presence of rotenoids, including deguelin, dehydrodeguelin, elliptone, 12a-hydroxyrotenone, rotenone and tephrosin, that have been reported from various parts of the plant (Ingham, 1983; Marston et al., 1984). The major rotenoids in the leaves are deguelin and rotenone (Irvine and Freyre, 1959), while other flavonoid constituents of

* Corresponding author at: Natural Resources Institute, University of Greenwich, Central Avenue, Chatham Maritime, Kent ME4 4TB, UK. Tel.: +44 208 332 5369; fax: +44 208 332 5310.
E-mail address: p.stevenson@kew.org (P.C. Stevenson).

0031-9422/$ - see front matter © 2012 Elsevier Ltd. All rights reserved.
http://dx.doi.org/10.1016/j.phytochem.2012.02.025

Author's personal copy

leaves are reported as rutin, isoquercitrin and quercetin 3-*O*-α-arabinopyranoside (Marston et al., 1984).

The potential livelihood impact of this multiple use plant is compelling, particularly for poorly-resourced small-scale farmers, and it is now cultivated widely on farm land in southern and eastern Africa. The aim of this study was to evaluate the chemical profile of *T. vogelii* with respect to insecticidal rotenoids, in order to establish whether some provenances were more suitable for promotion as pest control plants. Variation in the rotenoid content of leaves could influence the pesticidal efficacy of *T. vogelii*, since the activity of rotenoids is concentration dependent (Fang and Casida, 1999). The present study actually revealed a more serious issue relating to the use of *T. vogelii* since two chemical varieties were found, one containing rotenoids as the main type of flavonoid aglycones in the leaves (C1) and the other containing flavanones as the main aglycone type (C2).

In this paper we distinguish these chemotypes, investigate them both morphologically and by DNA sequence analysis, and provide a near complete description of their flavonoid chemistry, including the characterisation of five new flavanones (**19**, **20**, **22**, **24**, **25**) and a new dihydroflavonol (**23**) from *T. vogelii* C2. In addition we describe the flavonoid chemistry of *Tephrosia candida* DC., a species which we found had been confused with *T. vogelii* in the promotion of *Tephrosia* as a multi-use plant in Africa, and from which four new flavonol glycosides were obtained (**27**, **28**, **33**, **60**). Finally, the implications of these findings on the use of *T. vogelii* in crop protection and soil enrichment are considered.

2. Results and discussion

2.1. Comparative chemical analysis of T. vogelii chemotypes and T. candida

LC–UV–MS analysis of MeOH extracts of leaf material from 13 collections of *T. vogelii* being cultivated in Malawi revealed that among the samples there were two distinct profiles of flavonoid components (Fig. 1). The leaves of all plants contained a similar range of flavonoid glycosides (**1**–**13**) but the flavonoids occurring as free aglycones differed; these were either rotenoids (**14**–**18**), or prenylated flavanones (e.g. **19**, **22**–**26**) (see Fig. 2 and Section 2.3). Specimens were therefore assigned to either chemotype C1 (containing rotenoids) or C2 (containing flavanones), typified by two collections from the World Agroforestry Centre (ICRAF): *Stevenson 10091*, K (*T. vogelii* C1**)** and *Stevenson 10092*, K (*T. vogelii* C2**)**. Importantly, rotenoids could not be detected in leaves of *T. vogelii* C2.

The specimen *Stevenson 10092* (*T. vogelii* C2**)** was originally collected as *T. candida*, the name under which it had been cultivated at ICRAF and promoted as a multi-use plant. It was correctly identified here as *T. vogelii* by morphological and DNA sequence analysis (see Section 2.2). LC–UV–MS analysis of leaf extracts from two verified herbarium specimens of *T. candida* (*Keke 150*, K; *Tovey* sn, K) revealed a similar range of prenylated flavanones (e.g. **19**, **22**–**24**, **26**) to that observed in *T. vogelii* C2 but the structural variety of flavonol *O*-glycosides (**27**–**65**) was different to that of both *T. vogelii* chemotypes (Section 2.4). Rotenoids could not be detected in either herbarium specimen of *T. candida*.

2.2. Morphological and DNA sequence analysis

DNA sequence analysis and a detailed morphological comparison with verified herbarium specimens including *T. vogelii* (*Mankelow 93049*, K; *Balaka & Nachamba 1205*, K) and *T. candida* (*Keke 150*, K; *Tovey* sn, K) indicated that the two cultivated provenances from ICRAF were both *T. vogelii*. The main diagnostic morphological characters used to distinguish the two species within the Flora Zambesiaca area (Brummitt, 2007) are as follows:

(i) *T. vogelii:* Stems, leaf rachides and pods villous, stipules 11–20 × 2.5–4.5 mm, inflorescence bracts up to 16 × 13 mm, flowers usually in dense heads, calyces 14–20 (−24) mm long, pods 13–17 mm wide, lanate-tomentose.

(ii) *T. candida:* Stems, leaf rachides and pods pubescent to tomentose, stipules 4–10 × 0.8–1.2 mm, inflorescence bracts 3–6 × 0.5–0.8 mm, flowers usually in fairly dense racemes, calyces 4–6 mm long, pods 7–9 mm wide, closely appressed pubescent.

DNA sequencing of the nuclear internal transcribed spacer (ITS) and plastid *trnL-F* regions of a second collection of *Stevenson 10091* and *Stevenson 10092* (*GSileshi 001*, K and *GSileshi 002*, K respectively) showed that both sequences differed by only two nucleotides between the two specimens, in both ITS and *trnL-F*. In contrast, *GSileshi 001* and *GSileshi 002* show much more sequence divergence with *T. candida* (*Keke 150*); 39 and 39 different nucleotides in ITS, respectively, and 9 and 7 different nucleotides in *trnL-F*, respectively (Section 3.3).

2.3. Identification of flavonoids in T. vogelii chemotypes C1 and C2

The flavonoid glycosides detected in MeOH extracts of both *T. vogelii* C1 and C2 were identified by LC–UV–MS/MS methods (Section 3.5). Among these were quercetin 3-*O*-robinobioside (**1**), quercetin 3-*O*-rutinoside (**2**), quercetin 3-*O*-galactoside (**3**) quercetin 3-*O*-glucoside (**4**) and a quercetin 3-*O*-pentoside (**6**), the kaempferol analogues of these (**5**, **8**, **7, 9** and **12,** respectively), isorhamnetin 3-*O*-galactoside (**10**), isorhamnetin 3-*O*-glucoside (**11**) and an isorhamnetin 3-*O*-pentoside (**13**). The most abundant flavonoid glycosides were generally **3, 4** and **6** (Fig. 1). Compound **6** was identified by comparison with a standard as quercetin 3-*O*-α-arabinopyranoside (guaijaverin), in accordance with a previous report (Marston et al., 1984); the 3-*O*-pentosides of kaempferol and isorhamnetin detected (**12** and **13**) are therefore likely to be the 3-*O*-α-arabinopyranosides.

The major flavonoid aglycones present in MeOH extracts of leaves of *T. vogelii* C1 were the rotenoids deguelin (**17**) and tephrosin (**15**), both of which were reported previously from this species (Ingham, 1983; Marston et al., 1984). Isolation of these compounds allowed their structures to be confirmed by comparison of NMR data with literature values (Dagne et al., 1989; Ye et al., 2008). Also present in the extracts of C1, usually as more minor components, were sarcolobine (**14**), rotenone (**16**) and α-toxicarol (**18**); these identifications were similarly confirmed using NMR data (Andrei et al., 1997; Blaskó et al., 1989; Wangensteen et al., 2005). Sarcolobine (**14**) was known previously only from stem extracts of *Sarcolobus globosus* (Apocynaceae).

Flavonoid aglycones present in MeOH extracts of leaves of *T. vogelii* C2 were isolated by semi-preparative HPLC, which afforded **19**–**26** as amorphous off-white solids (Fig. 2). Spectroscopic and chiroptical analysis established the structures of **21** and **26** as the known compounds 5,7-dimethoxy-8-(3-hydroxy-3-methylbut-1*Z*-enyl)flavone (*Z*-tephrostachin) and (2*S*)-5-methoxy-6″,6″-dimethylpyrano[2″,3″:7,8]flavanone (obovatin 5-methyl ether), respectively (Andrei et al., 2000; Vleggaar et al., 1973). A complete set of ^{1}H and ^{13}C NMR assignments for **21** is given in Tables 1 and 2, in the absence of comparable literature data.

The planar structures and full assignment of the ^{1}H and ^{13}C NMR spectra of **19**, **20** and **22**–**25** were obtained using standard one- and two-dimensional (COSY, HSQC, and HMBC) datasets. The corresponding molecular formulae were confirmed from high resolution ESI-MS measurements (Sections 3.6–3.13). In the ^{1}H

Author's personal copy

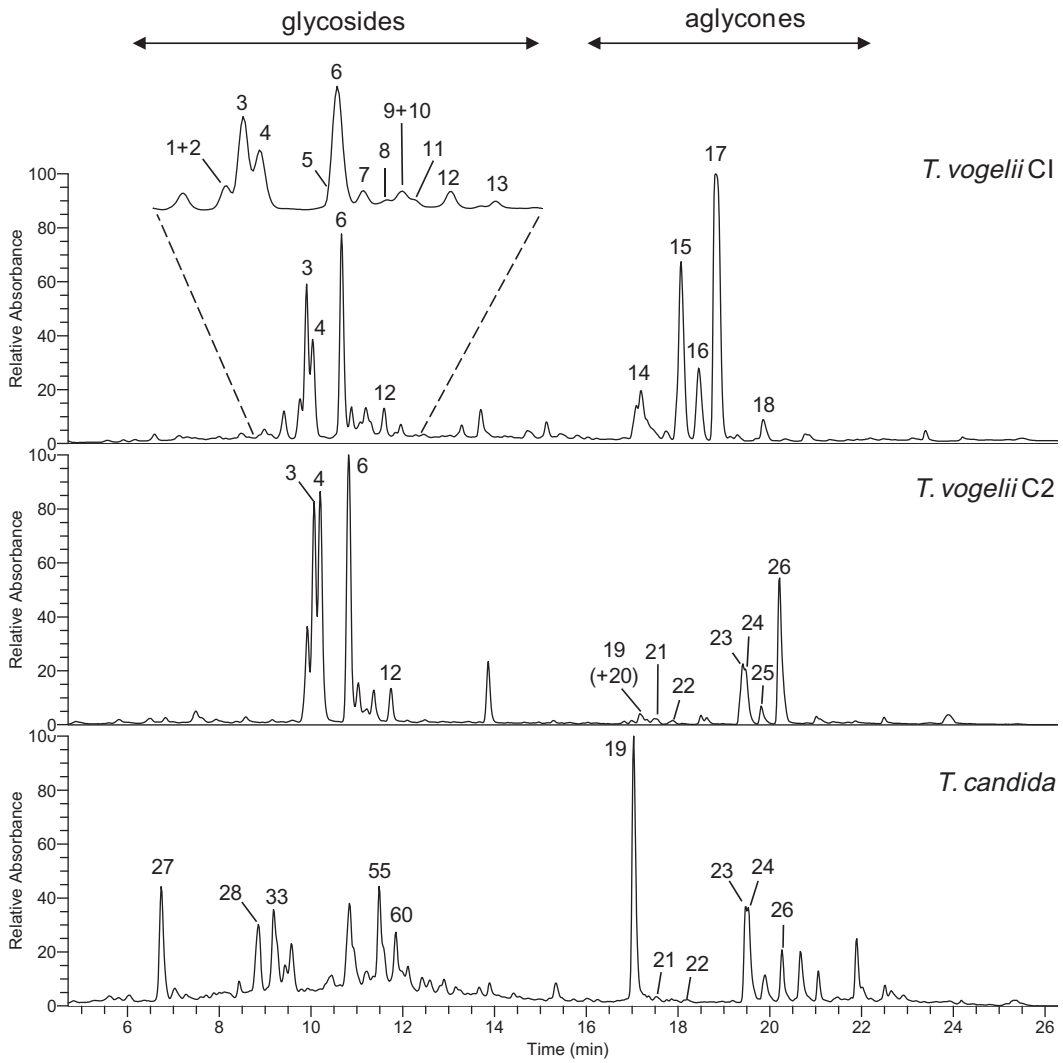

Fig. 1. UV spectrum maximum (320–500 nm) chromatograms from LC–UV–MS analyses of MeOH extracts of *Tephrosia vogelii* chemotype C1, *T. vogelii* chemotype C2, and *T. candida*. Peak identities given in text.

NMR spectra of **19**, **20**, **22**, **24**, and **25**, the characteristic chemical shift, multiplicity and *J*-values of the resonances assigned to H-2 and CH_2-3 indicated that these compounds were flavanones (Table 1). The ^{1}H NMR spectrum of **19** also contained resonances for an unsubstituted phenyl ring, which corresponded to the B-ring of the flavanone, and a singlet resonance at δ_H 6.16 (δ_C 89.0) assigned to H-6 of the A-ring from its correlations with the quaternary carbons C-5 (δ_C 162.0), C-7 (δ_C 161.9), C-8 (δ_C 108.0), and C-10 (δ_C 106.3) in the HMBC spectrum. The remaining resonances were those of two methoxy groups and a 3-hydroxy-3-methylbut-1*Z*-enyl substituent (Tables 1 and 2), the locations of which were established using HMBC data. For the prenyl chain, key correlations observed from H-1″ to C-7 and C-9, and from H-2″ to C-8, confirmed C-8 as the site of substitution. Similarly, the methoxy resonances correlated with C-5 and C-7. NOE correlations were also detected between the resonance of H-6 and those of 5-OMe and 7-OMe. Compound **19** was therefore 5,7-dimethoxy-8-(3-hydroxy-3-methylbut-1*Z*-enyl)flavanone, which has a pattern of substitution identical to that of the flavone *Z*-tephrostachin (**21**). The *E*-isomer of **19** was obtained previously as quercetol C from root extracts of *Tephrosia quercetorum* C. E. Wood (Gómez-Garibay et al., 1988). Negative and positive Cotton effects observed at 288 and 336 nm, respectively, in the CD spectrum of **19** indicated that it was present in the (2*S*)-configuration (Slade et al., 2005).

Compound **20** was obtained during isolation of the HPLC peak containing **19**; in crude extracts it was a very minor component by MS detection, showing poor chromatography. The ^{1}H and ^{13}C NMR spectra of **20** were similar to those of **19**, with the exception of those resonances corresponding to the prenyl substituent of each compound. In **20**, this was identified as a 3-methylbut-1,3-dienyl, rather than a 3-hydroxy-3-methylbut-1*Z*-enyl moiety. Correlations in the HMBC spectrum of **20** detected from H-1″ to C-7 and C-9, and from H-2″ to C-8, confirmed C-8 as the site of prenylation. The CD spectrum of **20** indicated that it possessed the (2*S*)-configuration, with negative and positive Cotton effects observed at 289 and 343 nm, respectively. Compound **20** was therefore (2*S*)-5,7-dimethoxy-8-(3-methylbut-1,3-dienyl)flavanone. A 5-demethyl analogue of the latter has been reported as tephroleocarpin B from the roots of *T. leiocarpa* A. Gray (Gómez-Garibay et al., 1991).

The ^{1}H and ^{13}C NMR spectra of **22** indicated that it was a derivative of obovatin 5-methyl ether (**26**) with a different B-ring structure. Instead of the unsubstituted phenyl ring of the latter, the resonances at δ_H 7.33 (2H, *d*, *J* = 8.5 Hz) and 6.87 (2H, *d*, *J* = 8.5 Hz) indicated the presence of 4′-OH substitution. The ^{1}H NMR spectrum of **22** was also similar to that of 5,4′-dihydroxy-6″,6″-dimethylpyrano[2″,3″:7,8]flavanone (citflavanone) acquired in $CDCl_3$ (Ito et al., 1988; Wu, 1989), except that a methoxy

Author's personal copy

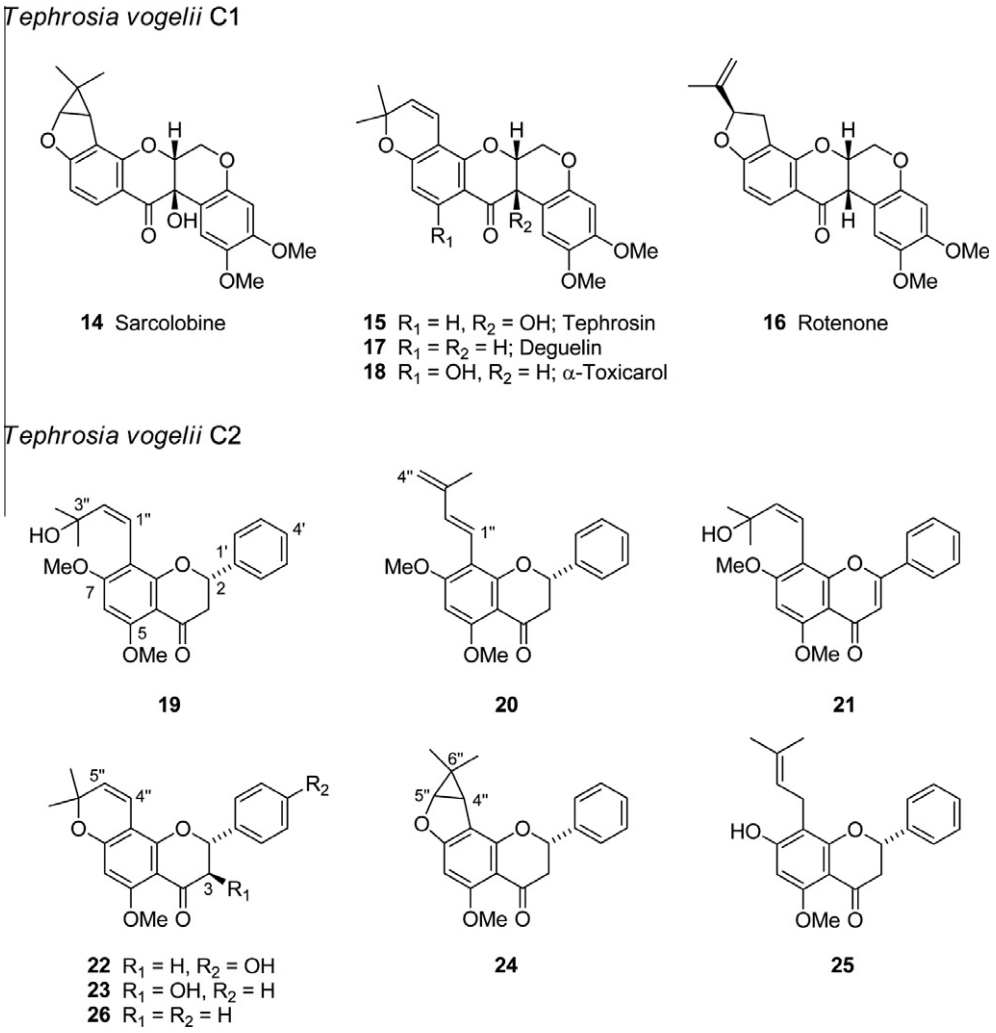

Fig. 2. Flavonoid aglycones of *Tephrosia vogelii* chemotypes C1 and C2.

Table 1
^{1}H NMR spectroscopic data (δ ^{1}H, *J* in Hz) for **19**–**25** ($CDCl_3$, 30 °C).

Atom	19	20	21	22	23	24	25
2	5.43 *dd* (12.5, 3.2)	5.48 *dd* (12.7, 3.2)		5.35 *dd* (13.2, 3.0)	5.02 *d* (12.1)	5.45 *dd* (12.3, 3.2)	5.41 *dd* (13.1, 2.9)
3	3.01 *dd* (16.6, 12.5)	3.01 *dd* (16.4, 12.7)	6.72 *s*	2.99 *dd* (16.6, 13.2)	4.39 *d* (12.1)	3.04 *dd* (16.5, 12.3)	2.98 *dd* (16.5, 13.1)
	2.87 *dd* (16.6, 3.2)	2.89 *dd* (16.4, 3.2)		2.89 *dd* (16.6, 3.0)		2.87 *dd* (16.5, 3.2)	2.83 *dd* (16.5, 2.9)
6	6.16 *s*	6.16 *s*	6.45 *s*	6.05 *s*	6.08 *s*	6.08 *s*	6.09 *s*
2′/6′	7.42 *m*	7.49 *m*	7.88 *m*	7.33 *d* (8.5)	7.57 *m*	7.46 *m*	7.45 *m*
3′/5′	7.40 *m*	7.42 *m*	7.50 *m*	6.87 *d* (8.5)	7.45 *m*	7.42 *m*	7.41 *m*
4′	7.36 *m*	7.33 *m*	7.50 *m*		7.42 *m*	7.38 *m*	7.36 *m*
5-OMe	3.92 *s*	3.963 *s*	4.02 *s*	3.89 *s*	3.92 *s*	3.87 *s*	3.87 *s*
7-OMe	3.95 *s*	3.960 *s*	3.99 *s*				
1″	5.96 *d* (12.4)	6.75 *d* (16.5)	6.21 *d* (12.3)				3.39 *d* (7.3)
2″	5.84 *d* (12.4)	7.24 *d* (16.5)	6.10 *d* (12.3)				5.26 *t* (7.3)
4″		4.97 *br s*		6.58 *d* (10.0)	6.54 *d* (10.0)	2.49 *d* (5.7)	1.76 *br s*
		4.94 *br s*					
5″				5.45 *d* (10.0)	5.46 *d* (10.0)	4.46 *d* (5.7)	
3″-Me		1.93 *s*					1.76 *br s*
gem-3″-Me	1.22 *s*		1.25 *s*				
gem-6″-Me				1.46 *s*	1.46 *s*	1.11 *s*	
				1.44 *s*	1.45 *s*	0.80 *s*	

resonance replaced that corresponding to 5-OH (Table 1). As expected, site selective excitation at δ_H 3.89 (5-OMe) in a one-dimensional NOE experiment gave a correlation to H-6 (δ_H 6.05). The CD spectrum of **22** showed negative and positive Cotton effects at 294 and 342 nm, respectively; its structure was therefore (2*S*)-4′-hydroxy-5-methoxy-6″,6″-dimethylpyrano[2″,3″:7,8]flavanone (citflavanone 5-methyl ether).

Compound **23** was also a derivative of **26** according to comparisons of NMR spectra. In this case, the difference in structure resided in the C-ring, which in the ^{1}H NMR spectrum of **23** was

Author's personal copy

Table 2
^{13}C NMR spectroscopic data (δ ^{13}C) for **19**–**25** ($CDCl_3$, 30 °C).

Atom	19	20	21	22	23	24	25
2	78.9	78.8	160.7	78.5	83.1	78.9	78.9
3	45.5	45.4	108.4	45.3	72.8	45.5	45.6
4	189.5	189.8	178.0	189.2	190.7	189.1	189.7
5	162.0	161.4	160.5	162.0	162.0	162.4	160.8
6	89.0	89.0	91.7	93.6	94.0	87.8	93.5
7	161.9	163.5	159.8	159.7	161.2	168.4	161.5
8	108.0	107.8	107.8	102.8	103.0	107.9	106.6
9	160.0	161.6	155.8	159.1	158.7	159.4	161.6
10	106.3	106.9	109.2	104.3	102.6	106.2	106.1
1′	138.7	139.0	131.7	130.9	136.8	139.0	139.1
2′/6′	126.1	125.8	126.0	127.8	127.4	126.2	125.9
3′/5′	128.8	128.7	128.9	115.3	128.6	128.7	128.7
4′	128.6	128.5	131.2	155.6	129.1	128.5	128.4
5-OMe	55.8	55.8		56.0	56.3	56.4	56.1
7-OMe	56.2	56.1					
1″	117.1	118.3	116.4				22.2
2″	141.5	134.8	142.9				121.5
3″	71.5	143.5	71.8				135.7
4″		116.1		115.8	115.6	29.6	25.5[a]
5″				126.0	126.6	73.2	
6″				77.8	78.4	15.1	
3″-Me		18.2					17.6[a]
gem-3″-Me	29.8		29.8				
gem-6″-Me				28.3	28.6	22.9	
				28.0	28.3	12.8	

[a] Assignments interchangeable.

represented by resonances at δ_H 5.02 (1H, *d*, *J* = 12.1 Hz) and 4.39 (1H, *d*, *J* = 12.1 Hz), corresponding to those of H-2 and H-3, respectively, of a dihydroflavonol. The ^{13}C resonances for C-2 and C-3 had chemical shift values typical for this class of flavonoid at δ_C 83.1 and 72.8, respectively (Fossen and Andersen, 2006). The absolute configuration of the dihydroflavonol was established using a combination of NMR and CD data (Slade et al., 2005). A value of $J_{2,3}$ = 12.1 Hz obtained from the ^{1}H NMR spectrum indicated that a *trans*-stereoisomer was present. In the CD spectrum, a positive Cotton effect observed at 342 nm defined the absolute configuration at C-2 as (2*R*). Thus compound **23** was (2*R*,3*R*)-3-hydroxy-5-methoxy-6″,6″-dimethylpyrano[2″,3″:7,8]flavanone, the dihydroflavonol equivalent of **26**. A regioisomer with linear rather than angular pyrano-functionalization of the A-ring was described as 3-hydroxy-5-methoxy-6″,6″-dimethylpyrano[2″,3″:7,6]flavanone from root extracts of *Lonchocarpus xuul* Lundell (Leguminosae), although the absolute configuration was not determined (Borges-Argáez et al., 2005).

The ^{1}H NMR spectrum of flavanone **24** contained resonances for an unsubstituted phenyl B-ring, an OMe group (δ_H 3.87) located at C-5, and an aromatic proton at δ_H 6.08 (δ_C 87.8) assigned to H-6. The remaining resonances comprised singlets at δ_H 0.80 and 1.11 (both 3H; correlated with δ_C 12.8 and 22.9, respectively by HSQC), corresponding to a *gem*-dimethyl group, and *J*-coupled doublets at δ_H 2.49 and 4.46 (both 1H, *J* = 5.7 Hz; correlated with δ_C 29.6 and 73.2, respectively). In the HMBC spectrum, correlations were detected between the resonances of the *gem*-dimethyl group and a quaternary carbon at δ_C 15.1, as well as to the proton-attached carbons at δ_C 29.6 and 73.2. Other important correlations were those from δ_H 2.49 to C-7 (δ_C 168.4) and C-9 (δ_C 159.4), δ_H 4.46 to C-7, and H-6 (δ_H 6.08) to C-5 (δ_C 162.4), C-7, C-8 (δ_C 107.9), and C-10 (δ_C 106.2). These correlations, and the chemical shifts of the aliphatic moiety were consistent with the presence of a dimethyldihydrocyclopropafurano group attached at O-7 and C-8 of the flavanone A-ring. This modified prenyl moiety is identical in structure to that which characterises the A-ring of sarcolobine (**14**) and the isoflavone, sarcolobone, which both occur in *Sarcolobus globosus* (Wangensteen et al., 2005), although the former was also present in *T. vogelii* C1. The subset of ^{1}H and ^{13}C resonances corresponding to this group in **24** were similar in terms of chemical shift and *J*-values to those reported for sarcolobine (**14**) and sarcolobone under similar solution conditions (Wangensteen et al., 2005). Although H-4″ and H-5″ of **24**, for which $J_{4'',5''}$ = 5.7 Hz, are *cis*-oriented, the absolute configurations at C-4″ and C-5″ were not determined. For the flavanone moiety, negative and positive Cotton effects observed in the CD spectrum at 290 and 321 nm, respectively, indicated that the (2*S*)-configuration was present. Thus **24** was (2*S*)-5-methoxy-6″,6″-dimethyl-4″,5″-dihydrocyclopropa[4″,5″]furano[2″,3″:7,8]flavanone.

Analysis of the ^{1}H NMR spectrum of flavanone **25** provided evidence for an unsubstituted phenyl B-ring, a methoxy group, and a prenyl group (Table 1). The methoxy group was located at C-5 according to its NOE correlation with the singlet resonance of H-6 at δ_H 6.09; similarly correlations were detected from the latter in HMBC data to C-5 (δ_C 160.8), C-7 (δ_C 161.5), C-8 (δ_C 106.6), and C-10 (δ_C 106.1). The prenyl group was at C-8 based on correlations detected in HMBC data between H-2″ and C-8, and CH_2-1″ to C-7, C-8, and C-9. In the corresponding CD spectrum, negative and positive Cotton effects were observed at 287 and 331 nm, respectively. Compound **25** was therefore (2*S*)-7-hydroxy-5-methoxy-8-prenylflavanone, which represents the immediate biosynthetic precursor of **26**.

2.4. Identification of flavonoids in *T. candida*

LC–MS/MS analysis of MeOH extracts of leaf material taken from a herbarium specimen of *T. candida* (*Keke 150*) indicated that flavonoid aglycones similar to those of *T. vogelii* C2 were present. However, the profile of flavonoid glycosides was different to that of both *T. vogelii* chemotypes (Fig. 1). In total, 41 flavonol glycosides (**5**, **8**, **27**–**65**) were detected in *T. candida* (Table 3) and assigned by LC–MS/MS methods (Section 3.5). Only two of these (**5** and **8**) occurred in *T. vogelii*. The flavonol glycosides of *T. candida* were based predominantly on 3,5,7,4′-tetrahydroxy-6-methoxyflavone (6-hydroxykaempferol 6-methyl ether; 6-methoxykaempferol) and included numerous acylated derivatives. Flavonol glycosides based on 3,5,7,4′-tetrahydroxy-6,3′-dimethoxyflavone (spinacetin), 3,5,7,3′,4′-pentahydroxy-6-methoxyflavone (patuletin) and kaempferol were also present.

The structures of three of the major non-acylated flavonoid glycosides (**27**, **28** and **33**) and one of the major acylated flavonoid glycosides (**60**) were determined by cryoprobe NMR spectroscopy using small amounts of the compounds isolated from herbarium material by HPLC (Fig. 3 and Section 3.4). The corresponding molecular formulae were determined using HRESIMS (Sections 3.14–3.17). The structure of **27** was elucidated using one-dimensional ^{1}H and site selective NOE, and two-dimensional COSY, HSQC and HMBC experimental data. Identification of the aglycone as 6-hydroxykaempferol 6-methyl ether was primarily based on its characteristic ^{1}H and ^{13}C NMR assignments (Merfort and Wendisch, 1987), as summarised in Table 4. In addition, correlations detected by HMBC from the singlet resonance of H-8 (δ_H 6.91) to C-6 (δ_C 134.3), C-7 (δ_C 156.8), C-9 (δ_C 153.5), and C-10 (δ_C 108.2), and from the OMe resonance at δ_H 3.87 (3H, *s*, δ_C 61.6) to C-6, confirmed the structure of the A-ring. Apart from the typical B-ring resonances of a kaempferol derivative, the remaining resonances in the ^{1}H and ^{13}C NMR spectra of **27** were those of four sugar residues, with anomeric protons appearing at δ_H 5.62 (1H, *d*, *J* = 7.8 Hz), 5.60 (1H, *d*, *J* = 1.8 Hz), 5.22 (1H, *d*, *J* = 1.8 Hz), and 4.51 (1H, *d*, *J* = 1.7 Hz). Full assignment of these resonances, including all multiplicities and *J*-values (Table 4), indicated that the sugars comprised one β-galactopyranosyl residue and three α-rhamnopyranosyl residues (Duus et al., 2000). One of the α-Rha*p* residues, designated Rha(III), was *O*-linked at C-7, according

Author's personal copy

Table 3
Flavonoids detected in a methanol extract of a herbarium specimen of *Tephrosia candida* (*Keke 150*) by LC–MS. Listed are the mean accurate masses and determined ionic formulae of $[M–H]^-$, HPLC retention times (t_R), relative peak height in the base ion chromatogram (Rel Pk Ht), aglycone identity and *O*-linked sugars at C-3 and C-7. Structural assignments (Det.) supported by data from NMR and MS[a].

No	t_R	$[M–H]^-$ (*m/z*)	$[M–H]^-$ (formula)	Rel. Pk. Ht (%)	Aglycone	C-3	C-7	Det.
27	6.64	915.2762	$C_{40}H_{51}O_{24}$	20.4	6-Methoxykaempferol	α-Rha-(1 → 2)-[α-Rha-(1 → 6)]-β-Gal-	α-Rha-	NMR
5	11.26	739.2103	$C_{33}H_{39}O_{19}$	0.5	Kaempferol	α-Rha-(1 → 6)-β-Gal-	α-Rha-	MS
28	11.31	769.2203	$C_{34}H_{41}O_{20}$	8.6	6-Methoxykaempferol	α-Rha-(1 → 6)-β-Gal-	α-Rha-	NMR
29	12.19	739.2100	$C_{33}H_{39}O_{19}$	2.2	Kaempferol	α-Rha-(1 → 2)-[α-Rha-(1 → 6)]-β-Gal-		MS
30	12.37	769.2216	$C_{34}H_{41}O_{20}$	0.2	6-Methoxykaempferol	α-Rha-(1 → 6)-β-Glc-	α-Rha-	MS
31	12.54	739.2098	$C_{33}H_{39}O_{19}$	0.3	6-Methoxykaempferol	α-Rha-(1 → ?)-Pen-	α-Rha-	MS
32	12.90	739.2097	$C_{33}H_{39}O_{19}$	0.7	Kaempferol	α-Rha-(1 → 2)-[α-Rha-(1 → 6)]-β-Glc-		MS
33	13.11	769.2202	$C_{34}H_{41}O_{20}$	16.4	6-Methoxykaempferol	α-Rha-(1 → 2)-[α-Rha-(1 → 6)]-β-Gal-		NMR
8	13.18	739.2083	$C_{33}H_{39}O_{19}$	tr	Kaempferol	α-Rha-(1 → 6)-β-Glc-		MS
34	13.70	769.2225	$C_{34}H_{41}O_{20}$	0.9	6-methoxykaempferol	α-Rha-(1 → 2)-[α-Rha-(1 → 6)]-β-Glc-		MS
35	14.28	799.2302	$C_{35}H_{43}O_{21}$	0.8	Spinacetin	α-Rha-(1 → 2)-[α-Rha-(1 → 6)]-β-Glc-[b]		MS
36	14.59	1077.3085	$C_{49}H_{57}O_{27}$	1.9	6-Methoxykaempferol	α-Rha-(1 → 2)-[α-Rha-(1 → 6)]-(4-*O*-*E*-caffeoyl-β-Gal)-	α-Rha-	MS
37	14.77	799.2307	$C_{35}H_{43}O_{21}$	4.5	Spinacetin	α-Rha-(1 → 2)-[α-Rha-(1 → 6)]-β-Gal-		MS
38	15.03	1077.3109	$C_{49}H_{57}O_{27}$	0.7	6-Methoxykaempferol	α-Rha-(1 → 2)-[α-Rha-(1 → 6)]-(3-*O*-caffeoyl-β-Gal)-	α-Rha-	MS
39	18.12	1061.3152	$C_{49}H_{57}O_{26}$	1.5	6-Methoxykaempferol	α-Rha-(1 → 2)-[α-Rha-(1 → 6)]-(3-*O*-*p*-coumaroyl-β-Gal)-	α-Rha-	MS
40	18.17	1061.3144	$C_{49}H_{57}O_{26}$	2.1	6-Methoxykaempferol	α-Rha-(1 → 2)-[α-Rha-(1 → 6)]-(4-*O*-*p*-coumaroyl-β-Gal)-	α-Rha-	MS
41	18.68	1061.3171	$C_{49}H_{57}O_{26}$	0.5	6-Methoxykaempferol	α-Rha-(1 → 2)-[α-Rha-(1 → 6)]-(3-*O*-*p*-coumaroyl-β-Gal)-	α-Rha-	MS
42	19.35	1077.3116	$C_{49}H_{57}O_{27}$	0.3	6-Methoxykaempferol	α-Rha-(1 → 2)-[α-Rha-(1 → 6)]-(4-*O*-*Z*-caffeoyl-β-Gal)-	α-Rha-	MS
43	19.48	1091.3274	$C_{50}H_{59}O_{27}$	0.6	6-Methoxykaempferol	α-Rha-(1 → 2)-[α-Rha-(1 → 6)]-(4-*O*-*E*-feruloyl-β-Gal)-	α-Rha-	MS
44	20.01	1091.3280	$C_{50}H_{59}O_{27}$	0.4	6-Methoxykaempferol	α-Rha-(1 → 2)-[(3-*O*-*E*-feruloyl)-α-Rha-(1 → 6)]-β-Gal-	α-Rha-	MS
45	20.10	931.2516	$C_{43}H_{47}O_{23}$	0.2	6-Methoxykaempferol	α-Rha-(1 → 2)-[α-Rha-(1 → 6)]-(3-*O*-caffeoyl-β-Gal)-		MS
46	20.80	931.2520	$C_{43}H_{47}O_{23}$	1.5	6-Methoxykaempferol	α-Rha-(1 → 2)-[α-Rha-(1 → 6)]-(3-*O*-caffeoyl-β-Gal)-		MS
47	22.44	1061.3181	$C_{49}H_{57}O_{26}$	1.1	6-Methoxykaempferol	α-Rha-(1 → 2)-[α-Rha-(1 → 6)]-(4-*O*-*p*-coumaroyl-β-Gal)-	α-Rha-	MS
48	23.13	915.2565	$C_{43}H_{47}O_{22}$	2.2	6-Methoxykaempferol	α-Rha-(1 → 2)-[α-Rha-(1 → 6)]-(3-*O*-*E*-*p*-coumaroyl-β-Gal)-		MS
49	23.35	915.2581	$C_{43}H_{47}O_{22}$	1.3	6-Methoxykaempferol	α-Rha-(1 → 2)-[α-Rha-(1 → 6)]-(3-*O*-*Z*-*p*-coumaroyl-β-Gal)-		MS
50	23.44	931.2534	$C_{43}H_{47}O_{23}$	0.5	Patuletin	α-Rha-(1 → 2)-α-[Rha-(1 → 6)]-(4-*O*-*p*-coumaroyl-β-Gal)-		MS
51	23.77	945.2694	$C_{44}H_{49}O_{23}$	0.6	6-Methoxykaempferol	α-Rha-(1 → 2)-[α-Rha-(1 → 6)]-(3-*O*-feruloyl-β-Gal)-		MS
52	24.35	931.2495	$C_{43}H_{47}O_{23}$	3.6	6-Methoxykaempferol	α-Rha-(1 → 2)-[α-Rha-(1 → 6)]-(4-*O*-*E*-caffeoyl-β-Gal)-		MS
53	24.78	945.2686	$C_{44}H_{49}O_{23}$	0.7	6-Methoxykaempferol	α-Rha-(1 → 2)-[(3-*O*-*E*-feruloyl)-α-Rha-6]-β-Gal-	α-Rha-	MS
54	27.41	931.2506	$C_{43}H_{47}O_{23}$	1.0	6-Methoxykaempferol	α-Rha-(1 → 2)-[α-Rha-(1 → 6)]-(4-*O*-*Z*-caffeoyl-β-Gal)-		MS
55	27.59	915.2558	$C_{43}H_{47}O_{22}$	5.9	6-Methoxykaempferol	α-Rha-(1 → 2)-[α-Rha-(1 → 6)]-(4-*O*-*E*-*p*-coumaroyl-β-Gal)-		MS
56	28.06	945.2663	$C_{44}H_{49}O_{23}$	1.6	Spinacetin	α-Rha-(1 → 2)-[α-Rha-(1 → 6)]-(4-*O*-*p*-coumaroyl-β-Gal)-		MS
57	28.27	945.2669	$C_{44}H_{49}O_{23}$	2.3	6-Methoxykaempferol	α-Rha-(1 → 2)-[α-Rha-(1 → 6)]-(4-*O*-*E*-feruloyl-β-Gal)-		MS
58	28.50	915.2583	$C_{43}H_{47}O_{22}$	1.0	Kaempferol	α-Rha-(1 → 2)-[(3-*O*-*E*-feruloyl)-α-Rha-(1 → 6)]-β-Gal-		MS
59	28.74	975.2780	$C_{45}H_{51}O_{24}$	0.3	6-Methoxykaempferol	α-Rha-(1 → 2)-[(3-*O*-*E*-sinapoyl)-α-Rha-(1 → 6)]-β-Gal-		MS
60	28.91	945.2668	$C_{44}H_{49}O_{23}$	6.0	6-Methoxykaempferol	α-Rha-(1 → 2)-[(3-*O*-*E*-feruloyl)-α-Rha-(1 → 6)]-β-Gal-		NMR
61	29.11	975.2812	$C_{45}H_{51}O_{24}$	0.5	Spinacetin	α-Rha-(1 → 2)-[α-Rha-(1 → 6)]-(4-*O*-feruloyl-β-Gal)-		MS
62	29.81	975.2771	$C_{45}H_{51}O_{24}$	1.6	Spinacetin	α-Rha-(1 → 2)-[(3-*O*-*E*-feruloyl)-α-Rha-(1 → 6)]-β-Gal-		MS
63	29.99	915.2574	$C_{43}H_{47}O_{22}$	2.7	6-Methoxykaempferol	α-Rha-(1 → 2)-[α-Rha-(1 → 6)]-(4-*O*-*Z*-*p*-coumaroyl-β-Gal)-		MS
64	33.28	945.2690	$C_{44}H_{49}O_{23}$	1.7	6-Methoxykaempferol	α-Rha-(1 → 2)-[(3-*O*-*Z*-feruloyl)-α-Rha-(1 → 6)]-β-Gal-		MS
65	33.53	975.2776	$C_{45}H_{51}O_{24}$	0.4	Spinacetin	α-Rha-(1 → 2)-[(3-*O*-*Z*-feruloyl)-α-Rha-(1 → 6)]-β-Gal-		MS

[a] Details of the procedure for assignment by MS are outlined in the methodology section.
[b] The primary glycosidic sugar, as Glc or Gal, in **35** and **37** was supported by both MS^n fragmentation of $[M–H]^-$ and $[M+Na]^+$ (Kite and Veitch, 2009, 2011), however the elution order is atypical of flavonol 3-*O*-rutinosides and 3-*O*-robinobiosides.

to the NOE correlation detected between H-8 and H-1 of Rha(III) at δ_H 5.60, and the long-range correlation observed from the latter to C-7 in the HMBC spectrum. Also detected by HMBC were correlations between H-1 of β-Gal*p* to C-3 of the aglycone (δ_C 134.7), H-2 of β-Gal*p* to C-1 of Rha(I), H-1 of Rha(I) to C-2 of β-Gal*p*, CH_2-6 of β-Gal*p* to C-1 of Rha(II), and H-1 of Rha(II) to C-6 of β-Gal*p*. These defined an *O*-linked α-Rha*p*(1 → 2)-[α-Rha*p*(1 → 6)]-β-Gal*p* residue at C-3 of the aglycone. Compound **27** was therefore 6-hydroxykaempferol 6-methyl ether 3-*O*-α-rhamnopyranosyl(1 → 2)[α-rhamnopyranosyl(1 → 6)]-β-galactopyranoside-7-*O*-α-rhamnopyranoside. The ^1H and ^{13}C NMR assignments for the sugar residues of the latter were similar to those reported for the corresponding glycoside of kaempferol (Kite et al., 2007).

Analysis of a comparable set of NMR data acquired for **28** indicated that it had a similar structure to **27**, except that Rha(I) was lacking (Table 4). The key correlations in the HMBC spectrum that defined the sites of glycosylation of the aglycone, and the interglycosidic linkage of the α-Rha*p*(1 → 6)-β-Gal*p* residue, were as described for **27**. Compound **28** was therefore 6-hydroxykaempferol 6-methyl ether 3-*O*-α-rhamnopyranosyl(1 → 6)-β-galactopyranoside-7-*O*-α-rhamnopyranoside.

NMR analysis of **33** and **60** was more limited than that carried out for **27** and **28** because of the lower concentrations of the samples. As such, assignment of the spectra of the former compounds was restricted to ^1H and proton-attached ^{13}C resonances only (Table 5). In LC–MS/MS analyses, MS^4 of $[M+H]^+$ of **33** and **60** confirmed that the aglycone was identical to that of **27** and **28** (Section 3.5). The singlet resonance of H-8 was shifted upfield in the ^1H NMR spectra of both **33** (δ_H 6.47) and **60** (δ_H 6.48), compared to **27** (δ_H 6.91) and **28** (δ_H 6.94). This indicated that in contrast to the latter, neither **33** nor **60** was glycosylated at C-7. Each compound contained three sugars comprising one β-Gal*p* residue and two α-Rha*p* residues. Comparison between the ^1H and ^{13}C resonance assignments of the glycosyl moieties of **33** and **60** (Table 5) with those of **27** (Table 4) confirmed that all were characterised by the same branched trisaccharide *O*-linked at C-3. On this basis **33** was 6-hydroxykaempferol 6-methyl ether 3-*O*-α-rhamnopyranosyl(1 → 2)[α-rhamnopyranosyl(1 → 6)]-β-galactopyranoside. As expected, correlations were observed in the HMBC spectrum of **33** from H-2 of Gal to C-1 of Rha(I), CH_2-6 of Gal to C-1 of Rha(II), H-1 of Rha(I) to C-2 of Gal, and H-1 of Rha(II) to C-6 of Gal. Although **60** was similarly glycosylated, several points of difference emerged from a comparison of its NMR spectra with those

Author's personal copy

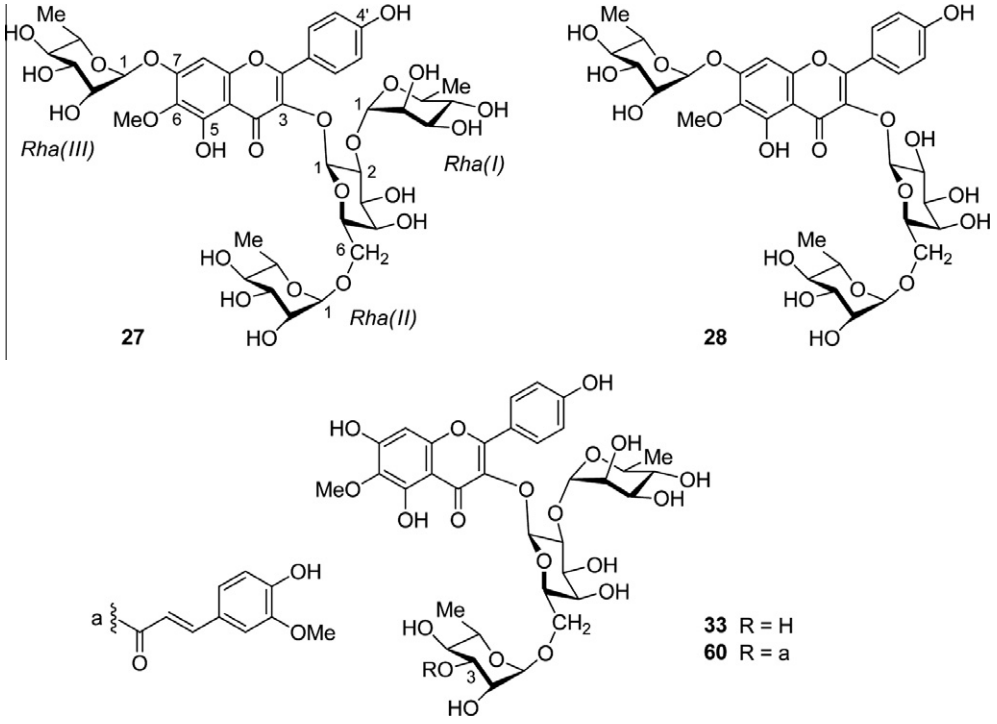

Fig. 3. Flavonol *O*-glycosides of *Tephrosia candida*.

of **33** (Table 5); an additional subset of resonances corresponding to an (*E*)-feruloyl group was present, H-3 of Rha(II) (the α-Rha*p* residue linked to C-6 of β-Gal*p*) was shifted downfield to δ_H 4.92 ($\Delta\delta$ = +1.43 ppm), and C-3 of Rha(II) to δ_C 75.4 ($\Delta\delta$ = +3.0 ppm). These observations were consistent with a structure for **60** of 6-hydroxykaempferol 6-methyl ether 3-*O*-α-rhamnopyranosyl(1 → 2)[(3-*O*-*E*-feruloyl)-α-rhamnopyranosyl(1 → 6)]-β-galactopyranoside. Compounds **27**, **28**, **33**, and **60** all represent new glycosidic combinations for 6-hydroxykaempferol 6-methyl ether.

2.5. Field survey of *T. vogelii* chemotypes

The flavonoid profiles of leaf material obtained from 13 collections of *T. vogelii* growing at farm locations in Malawi were compared using LC–UV–MS. Full details of the collection sites are provided in Table 6. The proportion of *T. vogelii* chemotype C2 was 23%. No correlation with white or purple flower colour was observed, indicating that this character cannot be used to distinguish chemotypes.

2.6. Implications for use of *T. vogelii* in pest control and for soil enrichment

T. vogelii is an important non-food plant species owing to its value in soil improvement through nitrogen fixation and as mineral rich green mulch. For these reasons it is cultivated extensively on fallow lands and inter-cropped with maize in southern Africa. *T. candida* is reported to have similar soil enriching properties and even to out-perform *T. vogelii* in this respect (Mafongoya and Kuntashula, 2005). However, this and many other studies of *T. candida* where the source material was obtained from World Agroforestry Centre, Nairobi, Kenya (e.g., Jama et al., 2008; Niang et al., 2002; Sileshi et al., 2005; Baijukya et al., 2006; Kamanga et al., 2010) appear to have been carried out using *T. vogelii* C2 incorrectly named as *T. candida*.

T. vogelii C1 is an effective botanical pest control alternative to synthetic pesticides and is reported by poor farmers across southern Africa to be a popular pesticide (Kamanula et al., 2011; Nyirenda et al., 2011) owing to the occurrence of the insecticidal rotenoids in the foliage. *T. candida* and *T. vogelii* C2, however, are not pesticidal as they lack rotenoids in their leaves. Obovatin 5-methyl ether (**26**) and *Z*-tephrostachin (**21**), major flavonoid aglycones of C2, have no reported insecticidal activity thus their occurrence is unlikely to confer pest control efficacy on C2. Preliminary biological evaluation of **26** against one target pest *Callosobruchus maculatus* showed no insect toxicity (P.C. Stevenson unpublished results). Thus, if agro-forestry extension services promote *T. vogelii* for soil improvement with the expectation that the materials will also provide farmers with an alternative pesticide, the correct chemotype must be selected. Chemical analysis is an important tool in the selection of elite plant material for indigenous uses (Sarasan et al., 2011). Further work is required to demonstrate unequivocally which material currently available to farmers is C1 and C2**,** and if any at all is *T. candida,* to ensure that farmers understand what the potential implications might be for the pesticidal use of the plants they are growing. Farmers should be discouraged from using C2 if they plan to use it for pest control.

3. Experimental section

3.1. General instrumentation

HREIMS measurements were made using a Thermo LTQ-Orbitrap XL mass spectrometer. Sample introduction was via a Thermo Accela LC system performing chromatographic separation of 5 μl injections on a Phenomenex Luna C18(2) column (150 mm × 3.0 mm i.d., 3 μm particle size) with a linear mobile phase gradient of 10–100% aqueous MeOH containing 0.1% formic acid over 20 min. Spectra were recorded in either positive or negative modes at 30,000 resolution.

NMR spectra were acquired in either $CDCl_3$ or MeOH-d_4 at 30 °C on Bruker Avance II 700 MHz or Avance 600 MHz instruments equipped with TCI-cryoprobes, or on a Bruker Avance 400 MHz instrument. Standard pulse sequences and parameters were used to obtain 1D ^{1}H, 1D ^{13}C, 1D site selective NOE (nuclear Overhauser

Author's personal copy

Table 4
^{1}H and ^{13}C NMR spectroscopic data for flavonol 3-*O*-glycoside-7-*O*-rhamnosides **27** and **28** (MeOH-d_4, 30 °C).

Atom		**27**		**28**	
		δ ^{1}H (*J* in Hz)	δ ^{13}C	δ ^{1}H (*J* in Hz)	δ ^{13}C
Aglycone	2		159.5		160.1
	3		134.7		135.7
	4		179.9		180.1
	5		nd[a]		nd[a]
	6		134.3		134.4
	7		156.8		157.0
	8	6.91 *s*	95.6	6.94 *s*	95.7
	9		153.5		153.6
	10		108.2		107.9
	1′		122.9		122.6
	2′/6′	8.10 *d* (8.9)	132.5	8.12 *d* (8.9)	132.7
	3′/5′	6.91 *d* (8.9)	116.4	6.90 *d* (8.9)	116.4
	4′		161.6		162.0
	6-OMe	3.87 *s*	61.6	3.87 *s*	61.4
3-*O*-Gal	1	5.62 *d* (7.8)	100.9	5.11 *d* (7.8)	105.2
	2	3.94 *dd* (9.5, 7.8)	77.7	3.79 *dd* (9.5, 7.8)	73.1
	3	3.70 *dd* (9.5, 3.5)	75.9	3.53 *dd* (9.5, 3.5)	75.1
	4	3.77 *dd* (3.5, 1.0)	70.9	3.77 *dd* (3.5, 1.1)	70.3
	5	3.63 *ddd* (6.9, 5.6, 1.0)	75.7	3.61 *ddd* (6.9, 5.5, 1.1)	75.7
	6	3.71 *dd* (10.6, 5.6)	67.5	3.72 *dd* (10.3, 5.5)	67.5
		3.46 *dd* (10.6, 6.9)		3.57 *dd* (10.3, 6.9)	
2^{Gal}-*O*-Rha(I)	1	5.22 *d* (1.8)	102.7		
	2	4.00 *dd* (3.4, 1.8)	72.6		
	3	3.79 *dd* (9.6, 3.4)	72.5		
	4	3.34 *t* (9.6)	74.2		
	5	4.04 *dd* (9.6, 6.2)	70.0		
	6	0.97 *d* (6.2)	17.7		
6^{Gal}-*O*-Rha(II)	1	4.51 *d* (1.7)	102.0	4.51 *d* (1.8)	102.0
	2	3.52 *dd* (3.4, 1.7)	72.3	3.56 *dd* (3.3, 1.8)	72.2
	3	3.47 *dd* (9.5, 3.4)	72.4	3.48 *dd* (9.5, 3.3)	72.4
	4	3.25 *t* (9.5)	74.0	3.27 *t* (9.5)	74.1
	5	3.51 *dd* (9.5, 6.2)	69.8	3.51 *dd* (9.5, 6.2)	69.8
	6	1.16 *d* (6.2)	18.1	1.18 *d* (6.2)	18.1
7-*O*-Rha(III)	1	5.60 *d* (1.8)	100.8	5.61 *d* (1.8)	100.7
	2	4.10 *dd* (3.5, 1.8)	71.9	4.10 *dd* (3.5, 1.8)	71.9
	3	3.91 *dd* (9.6, 3.5)	72.4	3.91 *dd* (9.6, 3.5)	72.3
	4	3.50 *t* (9.5)	73.7	3.50 *t* (9.5)	73.6
	5	3.68 *dd* (9.5, 6.2)	71.7	3.66 *dd* (9.6, 6.2)	71.6
	6	1.27 *d* (6.2)	18.3	1.27 *d* (6.2)	18.2

[a] Not detected (C-5 not assignable by inverse detection methods).

enhancement), 1D site selective ROE (rotating Overhauser enhancement), COSY (correlation spectroscopy), TOCSY (total correlation spectroscopy), HSQC (heteronuclear single quantum coherence), and HMBC (heteronuclear multiple bond correlation) spectra. Chemical shift referencing was carried out with respect to internal TMS at 0.00 ppm.

Optical rotation measurements (sodium D line, λ 589 nm, 22 °C) were made using a Perkin-Elmer 141 polarimeter with a 10 cm light path cylindrical cell of 1 ml volume. UV and CD spectra (22 °C, MeOH, 0.25 mg/ml) were acquired on an Applied Photophysics Ltd., Chirascan spectropolarimeter with the following parameters: 1 nm bandwidth, 1 nm step-size and a 0.5 s instrument time-per-point sampling; 2 mm and 0.5 mm cell path lengths were employed in the wavelength range 500–200 nm and all spectra were solvent baseline subtracted. All CD spectra were smoothed using the Savitsky-Golay method with a window factor between 4 and 20.

3.2. Plant material and standards

Collections of *T. vogelii* were made in October 2009 from 13 field sites across Malawi (Table 6). Herbarium vouchers for material collected from cultivated plants at the World Agroforestry Centre, Southern African Program, Chitedze, Lilongwe, Malawi – *Stevenson 10091* and *GSileshi 001* (ICRAF Acc No. 02976) and *Stevenson 10092* and *GSileshi 002* (ICRAF Acc No. 02972) have been deposited at the herbarium, Royal Botanic Gardens, Kew (K). Two verified herbarium specimens of *T. candida* (*Keke 150* and *Tovey* sn, K) were used for morphological, chemical and DNA sequence comparison.

A standard of rotenone was purchased from Sigma–Aldrich (Gillingham, Dorset, UK) while quercetin 3-*O*-α-arabinopyranoside (guaijaverin) was purchased from Apin Chemicals Ltd (Abingdon, UK). Other standards or extracts used to identify flavonol 3-*O*-glycosides are as listed by Kite and Veitch (2009, 2011).

3.3. DNA extraction and sequencing

Total genomic DNA was extracted using a modified version of the 2X CTAB method of Doyle and Doyle (1987). The total DNA was further purified for long-term storage in the DNA Bank at RBG Kew using a caesium chloride/ethidium bromide gradient (1.55 g/ml) followed by a dialysis procedure. The plastid region *trnL-F* (comprising the *trnL* intron and *trnL-F* intergenic spacer) was amplified using primers from Taberlet et al. (1991). Primers 17SE and 26SE from Sun et al. (1994) were used to amplify the nuclear internal transcribed spacer (ITS) region. The amplifications were conducted in 25 μl reactions, using 22.5 μl of Reddy PCR Master Mix (2.5 mM $MgCl_2$ for *trnL-F* and 1.5 mM for ITS; Thermo Fisher Scientific, Waltham, MA, USA), 0.9 μl of 0.4% bovine serum albumin, 0.3 μl of each primers (100 ng/μl) and 1 μl of template

Author's personal copy

Table 5
^{1}H and ^{13}C NMR spectroscopic data for flavonol 3-*O*-glycosides **33** and **60** (MeOH-d_4, 30 °C).

Atom		**33**		**60**	
		δ ^{1}H (*J* in Hz)	δ ^{13}C	δ ^{1}H (*J* in Hz)	δ ^{13}C
Aglycone	8	6.47 *s*	95.5	6.48 *s*	95.3
	2′/6′	8.06 *d* (8.9)	132.3	8.06 *d* (8.9)	132.3
	3′/5′	6.89 *d* (8.9)	116.3	6.90 *d* (8.9)	116.5
	6-OMe	3.88 *s*	61.0	3.85 *s*	61.0
3-*O*-Gal	1	5.60 *d* (7.7)	101.0	5.57 *d* (7.8)	101.0
	2	3.92 *dd* (9.6, 7.7)	77.7	3.94 *dd* (9.6, 7.8)	77.6
	3	3.69 *dd* (9.6, 3.5)	75.8	3.71 *dd* (9.6, 3.5)	75.7
	4	3.76 *dd* (3.5, 1.1)	70.8	3.81 *br d* (3.5)	70.8
	5	3.62 *ddd* (6.9, 5.6, 1.1)	75.5	3.67 *m*	75.3
	6	3.71 *dd* (10.5, 5.6)	67.3	3.75 *br d* (10.3)	67.2
		3.45 *dd* (10.5, 6.9)		3.47 *dd* (10.3, 6.9)	
2^{Gal}-*O*-Rha(I)	1	5.21 *d* (1.7)	102.7	5.23 *d* (1.7)	102.8
	2	4.00 *dd* (3.4, 1.7)	72.5	4.01 *dd* (3.4, 1.7)	72.5
	3	3.80 *dd* (9.5, 3.4)	72.4	3.83 *m*	72.3
	4	3.34 *t* (9.6)	74.2	3.35 *t* (9.6)	74.1
	5	4.06 *dd* (9.6, 6.2)	69.9	4.09 *dd* (9.6, 6.2)	69.9
	6	0.98 *d* (6.2)	17.5	1.00 *d* (6.2)	17.5
6^{Gal}-*O*-Rha(II)	1	4.51 *d* (1.8)	102.0	4.54 *d* (1.7)	101.9
	2	3.54 *dd* (3.4, 1.8)	72.2	3.77 *dd* (3.4, 1.7)	70.2
	3	3.49 *dd* (9.5, 3.4)	72.4	4.92 *dd* (9.7, 3.4)	75.4
	4	3.26 *t* (9.5)	74.0	3.56 *m*	71.4
	5	3.52 *dd* (9.5, 6.2)	69.7	3.66 *m*	70.2
	6	1.17 *d* (6.2)	17.9	1.22 *d* (6.2)	17.9
Feruloyl	α			6.37 *d* (16.0)	115.9
	β			7.64 *d* (16.0)	146.4
	2			7.20 *d* (1.8)	115.9
	5			6.81 *d* (8.4)	116.5
	6			7.09 *dd* (8.4, 1.8)	124.1
	3-OMe			3.90 *s*	56.6

Table 6
Location and chemotype data for samples of *T. vogelii* collected in Malawi.

Sample No.	Flower colour	Location	Alt. (m)	Date collected	Chemotype
BI-19309	White	Kakoko – Malivenji S: 10° 27.104′ E: 033° 58.081′	1306	08/01/2010	2
BI-20238	White	Lunyangwa S: 11° 25.650′ E: 034° 02.750′	1356	11/01/2010	1
BI-19310	Purple	Lumbwezi – Nchenachena S: 10° 43.830′ E: 034° 02.209′	1304	06/01/2010	2
BI-20239	White	Malepula V/H – Malivenji S: 11° 27.238′ E: 033° 57.161′	1302	08/01/2010	1
BI-20240	White	Maloto – Nchenachena S: 10° 45.714′ E: 034° 02.326′	1221	06/01/2010	1
BI-19311	White	Malepula – Malivenji S: 11° 27.269′ E: 033° 57.340′	1282	08/01/2010	2
BI-20241	Purple	Lunyangwa S: 11° 25.650′ E: 034° 02.750′	1356	11/01/2010	1
BI-20242	White	Choma S: 11° 17.811′ E: 034° 00.559′	1322	07/01/2010	1
BI-20243	White	Luweni – Nchenachena S: 10° 44.085′ E: 034° 02.464′	1279	06/01/2010	1
BI-20244	Purple	Maloto – Nchenachena S: 10° 45.564′ E: 034° 02.313′	1229	06/01/2010	1
BI-20245	White	Chawaye – Nchenachena S: 10° 46.096′ E: 034° 01.596′	1212	06/01/2010	1
BI-20246	White	Mkombezi S: 10° 56.464′ E: 033° 58.701′	1031	06/01/2010	1
BI-20247	White	Phwezi – Technical S: 10° 54.119′ E: 033° 02.236′	1023	06/01/2010	1

DNA. PCR conditions for both regions were as follow: initial denaturation at 94 °C for 2 min, followed by 28 cycles of 1 min at 94 °C, 1 min at 50 °C, 1.5 min at 72 °C, ending with a single final elongation of 4 min at 72 °C. Amplifications were performed on a GeneAmp PCR System 9700 (Applied Biosystems, Foster City, California, USA) and PCR products were purified using the Nucleospin® Extract II minicolumn kit (Macherey–Nagel, Düren). Cycle sequencing reactions were performed in 10 µl volume reactions containing 30–40 ng of PCR products, 0.5 µl BigDye® Terminator Cycle Sequencing kit (version 3.1; Applied Biosystems) and the same primers as for PCR. Cycle sequencing products were purified following the manufacturer's protocols and complementary strands were sequenced on an ABI 3730 automated sequencer. Sequencher 4.5 (Gene Codes Corp., Ann Arbor, MI, U.S.A.) was used to assemble complementary strands and verify software base-calling. The alignment was performed by eye in PAUP* (version 4.0b10; Swofford, 2002); sequences are available from GenBank (ITS, HE681569–HE681571; *trnL-F*, JQ712595-JQ712597).

3.4. Extraction, analysis, and isolation of flavonoids

Leaf material of *T. vogelii* samples was air dried for a week at room temperature, ground using a coffee mill, and 20 g extracted in MeOH for 24 h at room temperature. Each extract was filtered through Whatman grade 1 paper and an aliquot of the filtrate passed through a 0.45 µm nylon acrodisc filter. Routine LC–MS analysis of the filtered samples was carried out using a Waters Alliance system with a ZQ LC–MS detector on a Phenomenex Luna C18(2) column (150 × 4.0 mm i.d., 5 µm particle size) operating under gradient conditions, with A = MeOH, B = H_2O, C = 1% HCO_2H in MeCN; A = 0%, B = 90% at *t* = 0 min; A = 90%, B = 0% at *t* = 20 min; A = 90%, B = 0% at *t* = 30 min; A = 0%, B = 90% at *t* = 31 min; column temperature 30 °C and flow rate of 0.5 ml/min.

For flavonoid isolation from *T. vogelii* C1 and C2, the original MeOH extracts from 20 g leaves of each chemotype were taken to dryness using rotary evaporation, redissolved in 10 ml MeOH, and passed through 0.45 µm nylon acrodisc filters prior to HPLC.

Author's personal copy

Isolation was carried out on a Waters system (600E pump and 996 PDA detector) using a Spherisorb ODS2 column (250 mm × 10 mm i.d., 5 μm particle size) with a gradient elution program based on A = MeOH and B = H_2O; A = 25% at t = 0 min, A = 100% at t = 20 min, and A = 100% at t = 40 min; column temperature 30 °C and flow rate 4.7 ml/min. *T. vogelii* C1 yielded **14** (0.8 mg; t_R = 18.3 min), **15** (3.5 mg; t_R = 19.7 min), **17** (9.0 mg; t_R = 20.6 min) and **18** (0.8 mg; t_R = 21.6 min). Using the same gradient elution program *T. vogelii* C2 yielded **19 + 20** (2.6 mg; t_R = 18.3 min), **21** (1.5 mg; t_R = 18.9 min), **22** (1.5 mg; t_R = 19.5 min), **23 + 24** (2.5 mg; t_R = 20.5 min), **25** (21.5 mg; t_R = 20.5 min) and **26** (15.0 mg; t_R = 23.0 min). Final separation of coeluting components was achieved using isocratic conditions (55% MeOH) to give **19** (0.9 mg), **20** (0.25 mg), **23** (1.4 mg) and **24** (0.6 mg).

Flavonoid glycosides were isolated from a methanol extract of *T. candida* (*Keke 150*) (1 g) using the same HPLC instrumentation and column, but with a gradient elution program based on A = MeOH, B = H_2O, C = MeCN with 1% formic acid; A = 0% and B = 90% at t = 0 min, A = 90% and B = 0% at t = 20 min; column temperature 30 °C and flow rate 4.7 ml/min. Where required, an additional step using isocratic conditions (25% MeOH) was employed to improve the separation of near-coeluting components. These methods yielded **27** (1.7 mg), **28** (0.6 mg), **33** (0.5 mg), and **60** (0.3 mg).

3.5. Structural assignment of flavonol glycosides by LC–MS/MS

MeOH extacts of field collected *T. vogelii* and a herbarium specimen of *T. candida* (*Keke 150*) were analysed by LC–MS/MS using the orbitrap system described in Section 3.1. However for the *T. candida* extract, high resolution chromatography was performed on 2 μl injections using a Phenomenex Kinetex column (150 mm × 2.1 mm i.d., 2.6 μm particle size) with a 400 μl/min mobile phase gradient of 90:0:10 to 50:40:10 (water/methanol/acetonitrile +1% formic acid) over 40 min. Repeated analyses were performed to obtain MS^n data on $[M+H]^+$, $[M+Na]^+$ and $[M-H]^-$ either using automatic ion selection or manual programming to fragment selected ions, and recording either low resolution or 7000 resolution spectra. MS^1 data on $[M-H]^-$ were acquired at 30,000 resolution. High resolution data generally had a mass accuracy error of less than 2 ppm.

Quercetin, kaempferol or isorhamnetin aglycones of flavonol glycosides were identified by comparing the CID spectrum of $[A+H]^+$ with that of in-house library MS^2 spectra. Methylated aglycones of flavonol glycosides were assigned from the m/z value of $[A+H]^+$ following MS^2 of $[M+H]^+$ and comparing the CID spectrum of $[(A+H)-15]^+$, obtained by MS^4 analysis of $[M+H]^+$, with that of the equivalent spectrum from either **33** (a glycoside of 6-methoxykaempferol for which the structure was determined by NMR), glycosides of patuletin (3,5,7,3′,4′-pentahydroxy-6-methoxyflavone) assigned in an LC–MS analysis of an extract of *Spinacea*, or a standard of spinacetin (3,5,7,4′-tetrahydroxy-6,3′-dimethoxyflavone).

The structures of the di- and trisaccharides assumed to be linked at C-3 of the aglycone in the non-acylated flavonol glycosides were determined by the methods of Kite and Veitch (2009, 2011), except for the glycosyl group of **31** for which lack of comparative data precluded assignment beyond it being a 3-*O*-rhamnosylpentoside. An additional Rha, assumed to be at C-7, was assigned when high resolution MS^2 of $[M-H]^-$ indicated a single major loss of $C_6H_{10}O_4$. The anomeric configurations of sugars were also assumed to be those found in naturally occurring flavonol glycosides.

For flavonol glycosides bearing an acylated trisaccharide, the structure of the trisaccharide was determined by applying the negative ion methods of Kite and Veitch (2009) following removal of the acyl group by MS^2 (or MS^3 for 7-*O*-rhamnosides) from $[M-H]^-$. The molecular formula of this acyl group loss, determined by high resolution scanning, was used to assign it as coumaroyl, caffeoyl or feruloyl. Evidence for locating the acylation position to be at either C-3 or C-4 of Gal or C-3 of 6^{Gal}-*O*-Rha was obtained by comparing MS^n spectra of $[M+Na]^+$ with those of a variety of acylated flavonol glycosides isolated from two other Leguminosae genera, *Cladrastis* (Kite et al., 2011) and *Onobrychis* (Veitch et al., 2011), although it should be stressed that comparative MS^n data for all possible acylation positions of Rha-(1 → 2)-[Rha-(1 → 6)]-hexosides was not available. Specifically, acyl substitution at C-3 of Gal was revealed by the double loss of the acyl group and the aglycone following MS^2 of $[M+Na]^+$ (or MS^3 for 7-*O*-rhamnosides). Loss of the acyl group was not observed when the acyl substitution was at C-4 of Gal or C-3 of 6^{Gal}-*O*-Rha. These two substitution positions could be distinguished by differences in the CID spectra of the Rha-loss ion from the sodiated glycosyl group $[(M+Na)-aglycone]^+$. Additionally, substitution at C-3 of 6^{Gal}-*O*-Rha was revealed by the presence of an abundant $[AcylRha+H]^+$ fragment in the MS^2 of $[M+H]^+$.

The *E*- and *Z*-forms of the acyl group substituted at C-4 of Gal could be assigned from the relative abundance of an ion resulting from the neutral loss of 88 Da from the Rha-loss ion of the sodiated glycosyl group (G.C. Kite, unpublished observations on analogous compounds from *Cladrastis*). This ion was at greater relative abundance in the spectrum derived from the sodiated acylglycosyl group containing the *E*-form, but assignment required that both *E*- and *Z*- forms were located so as to compare relative abundances. MS^n analysis of $[M+Na]^+$ of **60** and **64** suggested that *E*- and *Z*-forms of the acyl group substituted at C-3 of Rha could also be differentiated. A minor ion at m/z 389 (which did not include the acyl group) was generated following CID of the sodiated acylglycosyl group if the acyl group was in the *E*-form but was absent if the acyl group was in the *Z*-form. Also an $[(acyl\text{-}rhamnose)+Na]^+$ fragment (m/z 363 for acyl = feruloyl) in the CID spectrum of the Rha-loss ion generated from the sodiated acylglycosyl group was at greater relative abundance if the acyl group was in the *Z*-form rather than the *E*-form. These trends were extrapolated for compounds containing different aglycones or acyl groups. *E*- and *Z*-forms of the acyl group substituted at C-3 of Gal could not be distinguished by mass spectral characteristics.

3.6. (2S)-5,7-Dimethoxy-8-(3-hydroxy-3-methylbut-1Z-enyl)flavanone (= Z-quercetol C) (**19**)

Off white solid; UV (MeOH) λ_{max} nm: 287, 321; CD $\Delta\varepsilon_{288}$ −6.866, $\Delta\varepsilon_{336}$ +3.451 (MeOH; c 0.225); ^{1}H NMR, see Table 1; ^{13}C NMR, see Table 2; HRESIMS m/z: 369.1696 $[M+H]^+$ (calc. for $C_{22}H_{25}O_5^+$, 369.1696).

3.7. (2S)-5,7-Dimethoxy-8-(3-methylbut-1,3-dienyl)flavanone (= tephroleocarpin B 5-methyl ether) (**20**)

Off white solid; UV (MeOH) λ_{max} nm: 271, 292sh, 312sh; CD $\Delta\varepsilon_{289}$ −1.358, $\Delta\varepsilon_{343}$ +0.403 (MeOH; c 0.125); ^{1}H NMR, see Table 1; ^{13}C NMR, see Table 2; HRESIMS m/z: 351.1593 $[M+H]^+$ (calc. for $C_{22}H_{23}O_4^+$, 351.1591).

3.8. 5,7-Dimethoxy-8-(3-hydroxy-3-methylbut-1Z-enyl)flavone (= Z-tephrostachin) (**21**)

Off white solid; UV (MeOH) λ_{max} nm: 269, 337; ^{1}H NMR, see Table 1; ^{13}C NMR, see Table 2; HRESIMS m/z: 367.1542 $[M+H]^+$ (calc. for $C_{22}H_{23}O_5^+$, 367.1540).

Author's personal copy

3.9. (2S)-4′-Hydroxy-5-methoxy-6″,6″-dimethylpyrano[2″,3″:7,8]flavanone (= citflavanone 5-methyl ether) (**22**)

Off white solid; UV (MeOH) λ_{max} nm: 260sh, 269, 293sh, 344sh; CD $\Delta\varepsilon_{294}$ −3.724, $\Delta\varepsilon_{342}$ +1.202 (MeOH; *c* 0.833); ^{1}H NMR, see Table 1; ^{13}C NMR, see Table 2; HRESIMS *m*/*z*: 353.1384 $[M+H]^+$ (calc. for $C_{21}H_{21}O_5^+$, 353.1383).

3.10. (2R,3R)-3-Hydroxy-5-methoxy-6″,6″-dimethylpyrano[2″,3″:7,8]flavanone (**23**)

Off white solid; UV (MeOH) λ_{max} nm: 261sh, 270, 295, 345; $[\alpha]_D^{22}$ −25.7° (*c* 0.07, MeOH); CD $\Delta\varepsilon_{300}$ −6.881, $\Delta\varepsilon_{342}$ +1.175 (MeOH; *c* 0.28); ^{1}H NMR, see Table 1; ^{13}C NMR, see Table 2; HRESIMS *m*/*z*: 353.1387 $[M+H]^+$ (calc. for $C_{21}H_{21}O_5^+$, 353.1383).

3.11. (2S)-5-Methoxy-6″,6″-dimethyl-4″,5″-dihydrocyclopropa[4″,5″]furano[2″,3″:7,8]flavanone (**24**)

Off white solid; UV (MeOH) λ_{max} nm: 272, 293, 332; CD $\Delta\varepsilon_{290}$ −9.984, $\Delta\varepsilon_{321}$ +5.131 (MeOH; *c* 0.30); ^{1}H NMR, see Table 1; ^{13}C NMR, see Table 2; HRESIMS *m*/*z*: 337.1437 $[M+H]^+$ (calc. for $C_{21}H_{21}O_4^+$, 337.1434).

3.12. (2S)-7-Hydroxy-5-methoxy-8-prenylflavanone (**25**)

Off white solid; UV (MeOH) λ_{max} nm: 287, 325sh; CD $\Delta\varepsilon_{287}$ −22.014, $\Delta\varepsilon_{331}$ +8.761 (MeOH; *c* 1.167); ^{1}H NMR, see Table 1; ^{13}C NMR, see Table 2; HRESIMS *m*/*z*: 339.1591 $[M+H]^+$ (calc. for $C_{21}H_{23}O_4^+$, 339.1591).

3.13. (2S)-5-Methoxy-6″,6″-dimethylpyrano[2″,3″:7,8]flavanone (= obovatin 5-methyl ether) (**26**)

Off white solid; UV (MeOH) λ_{max} nm: 259sh, 269, 294, 346; $[\alpha]_D^{22}$ −65.6° (*c* 0.63, MeOH); CD $\Delta\varepsilon_{299}$ −9.716, $\Delta\varepsilon_{340}$ +2.910 (MeOH; *c* 0.252); ^{1}H and ^{13}C NMR, in agreement with literature values (Andrei et al., 2000); HRESIMS *m*/*z*: 337.1430 $[M+H]^+$ (calc. for $C_{21}H_{21}O_4^+$, 337.1434).

3.14. 6-Hydroxykaempferol 6-methyl ether 3-*O*-α-rhamnopyranosyl(1 → 2)[α-rhamnopyranosyl(1 → 6)]-β-galactopyranoside-7-*O*-α-rhamnopyranoside (**27**)

Pale yellow solid; UV (LC–PDA) λ_{max} nm: 269, 337; ^{1}H and ^{13}C NMR, see Table 4; HRESIMS *m*/*z*: 915.2762 $[M-H]^-$ (calc. for $C_{40}H_{51}O_{24}^-$, 915.2776).

3.15. 6-Hydroxykaempferol 6-methyl ether 3-*O*-α-rhamnopyranosyl(1 → 6)-β-galactopyranoside-7-*O*-α-rhamnopyranoside (**28**)

Pale yellow solid; UV (LC–PDA) λ_{max} nm: 269, 337; ^{1}H and ^{13}C NMR, see Table 4; HRESIMS *m*/*z*: 769.2203 $[M-H]^-$ (calc. for $C_{34}H_{41}O_{20}^-$, 769.2197).

3.16. 6-Hydroxykaempferol 6-methyl ether 3-*O*-α-rhamnopyranosyl(1 → 2)[α-rhamnopyranosyl(1 → 6)]-β-galactopyranoside (**33**)

Pale yellow solid; UV (LC–PDA) λ_{max} nm: 269, 337; ^{1}H and ^{13}C NMR, see Table 5; HRESIMS *m*/*z*: 769.2202 $[M-H]^-$ (calc. for $C_{34}H_{41}O_{20}^-$, 769.2197).

3.17. 6-Hydroxykaempferol 6-methyl ether 3-*O*-α-rhamnopyranosyl(1 → 2)[(3-*O*-*E*-feruloyl)-α-rhamnopyranosyl(1 → 6)]-β-galactopyranoside (**60**)

Pale yellow solid; UV (LC–PDA) λ_{max} nm: 270, 298sh, 329; ^{1}H and ^{13}C NMR, see Table 5; HRESIMS *m*/*z*: 945.2668 $[M-H]^-$ (calc. for $C_{44}H_{49}O_{23}^-$, 945.2670).

Acknowledgements

We thank the Biomedical NMR Centre, National Institute for Medical Research, Mill Hill, London, for access to high-field NMR instrumentation, Drs. Tam Bui and Alex Drake, Pharmaceutical Optical & Chiroptical Spectroscopy Centre, Department of Pharmacy, King's College, London, for chiroptical data, and Sian Evans, RBG Kew, for help with the production of DNA sequences. This work was funded partly from a McKnight Foundation grant to S.P.N, S.R.B. and P.C.S. and an EU 9th European Development Fund grant to P.C.S. The contents of this document are the sole responsibility of the authors and can under no circumstances be regarded as reflecting the position of the McKnight Foundation or the European Union.

References

Andrei, C.C., Viera, P.C., Fernandes, J.B., da Silva, M., Fo, E.R., 1997. Dimethylchromene rotenoids from *Tephrosia candida*. Phytochemistry 46, 1081–1085.

Andrei, C.C., Ferreira, D.T., Faccione, M., de Moraes, L.A.B., de Carvalho, M.G., Braz-Filho, R., 2000. C-prenylflavonoids from roots of *Tephrosia tunicata*. Phytochemistry 55, 799–804.

Baijukya, F.P., de Ridder, N., Giller, K.E., 2006. Nitrogen release from decomposing residues of leguminous cover crops and their effect on maize yield on depleted soils of Bukoba District, Tanzania. Plant Soil 279, 77–93.

Blaskó, G., Shieh, H.-L., Pezzuto, J.M., Cordell, G.A., 1989. ^{13}C-NMR spectral assignment and evaluation of the cytotoxic potential of rotenone. J. Nat. Prod. 52, 1363–1366.

Borges-Argáez, R., Díaz, M.E.P., Waterman, P.G., Peña-Rodríguez, L.M., 2005. Additional flavonoids from *Lonchocarpus yucatanensis* and *L. xuul*. J. Braz. Chem. Soc. 16, 1078–1081.

Brummitt, R.K., 2007. Genus 19. *Tephrosia* Pers. In: Timberlake, J.R., Polhill, R.M., Pope, G.V., Martins, E.S. (Eds.), Flora Zambesiaca, vol. 3, Part 3. Royal Botanic Gardens, Kew, pp. 186–187.

Burkill, H.M., 1995. The Useful Plants of West Tropical Africa, vol. 3, second ed. Royal Botanic Gardens, Kew, pp. 460–462.

Dagne, E., Yenesew, A., Waterman, P.G., 1989. Flavonoids and isoflavonoids from *Tephrosia fulvinervis* and *Tephrosia pentaphylla*. Phytochemistry 28, 3207–3210.

Doyle, J.J., Doyle, J.L., 1987. Hybridization in *Claytonia* – morphology, fertility, and nuclear ribosomal genes. Am. J. Bot. 74, 701–702.

Duus, J.Ø., Gotfredsen, C.H., Bock, K., 2000. Carbohydrate structural determination by NMR spectroscopy: modern methods and limitations. Chem. Rev. 100, 4589–4614.

Fang, N.B., Casida, J.E., 1999. Cubé resin insecticide: identification and biological activity of 29 rotenoid constituents. J. Agric. Food Chem. 47, 2130–2136.

Fossen, T., Andersen, Ø.M., 2006. Spectroscopic techniques applied to flavonoids. In: Andersen, Ø.M., Markham, K.R. (Eds.), Flavonoids: Chemistry, Biochemistry and Applications. CRC Press, Boca Raton, pp. 37–142.

Gómez-Garibay, F., Quijano, L., Calderón, J.S., Morales, S., Ríos, T., 1988. Prenylflavanols from *Tephrosia quercetorum*. Phytochemistry 27, 2971–2973.

Gómez-Garibay, F., Quijano, L., Ríos, T., 1991. Flavanones from *Tephrosia leiocarpa*. Phytochemistry 30, 3832–3834.

Ingham, J.L., 1983. Naturally occurring isoflavonoids (1855–1981). Prog. Chem. Org. Nat. Prod. 43, 1–266.

Irvine, J.E., Freyre, R.H., 1959. Source materials for rotenone – occurrence of rotenoids in some species of the genus *Tephrosia*. J. Agric. Food Chem. 7, 106–107.

Ito, C., Mizuno, T., Matsuoka, M., Kimura, Y., Sato, K., Kajiura, I., Omura, M., Ju-ichi, M., Furukawa, H., 1988. A new flavonoid and other new components from *Citrus* plants. Chem. Pharm. Bull. 36, 3292–3295.

Jama, B.A., Mutegi, J.K., Njui, A.N., 2008. Potential of improved fallows to increase household and regional fuelwood supply: evidence from western Kenya. Agroforestry Syst. 73, 155–166.

Kamanga, B.C.G., Waddington, S.R., Robertson, M.J., Giller, K.E., 2010. Risk analysis of maize-legume crop combinations with smallholder farmers varying in resource endowment in central Malawi. Exp. Agric. 46, 1–21.

Kamanula, J., Sileshi, G.W., Belmain, S.R., Sola, P., Mvumi, B.M., Nyirenda, G.K.C., Nyirenda, S.P., Stevenson, P.C., 2011. Farmers' insect pest management practices

Author's personal copy

and pesticidal plant use in the protection of stored maize and beans in Southern Africa. Int. J. Pest Manage. 57, 41–49.
Kite, G.C., Veitch, N.C., 2009. Assigning glucose or galactose as the primary glycosidic sugar in 3-*O*-mono-, di- and triglycosides of kaempferol using negative ion electrospray and serial mass spectrometry. Rapid Commun. Mass Spectrom. 23, 3125–3132.
Kite, G.C., Veitch, N.C., 2011. Identification of common glycosyl groups of flavonoid *O*-glycosides by serial mass spectrometry of sodiated species. Rapid Commun. Mass Spectrom. 25, 2579–2590.
Kite, G.C., Stoneham, C.A., Veitch, N.C., 2007. Flavonol tetraglycosides and other constituents from leaves of *Styphnolobium japonicum* (Leguminosae) and related taxa. Phytochemistry 68, 1407–1416.
Kite, G.C., Rowe, E.R., Lewis, G.P., Veitch, N.C., 2011. Acylated flavonol tri- and tetraglycosides in the flavonoid metabolome of *Cladrastis kentukea* (Leguminosae). Phytochemistry 72, 372–384.
Mafongoya, P.L., Kuntashula, E., 2005. Participatory evaluation of Tephrosia species and provenances for soil fertility improvement and other uses using farmer criteria in eastern Zambia. Exp. Agric. 41, 69–80.
Marston, A., Msonthi, J.D., Hostettmann, K., 1984. On the reported molluscicidal activity from *Tephrosia vogelii* leaves. Phytochemistry 23, 1824–1825.
Merfort, I., Wendisch, D., 1987. Flavonoidglycoside aus *Arnica montana* und *Arnica chamissonis*. Planta Med. 53, 434–437.
Neuwinger, H.D., 2004. Plants used for poison fishing in tropical Africa. Toxicon 44, 417–430.
Niang, A.I., Amadalo, B.A., de Wolf, J., Gathumbi, S.M., 2002. Species screening for short-term planted fallows in the highlands of western Kenya. Agroforestry Syst. 56, 145–154.
Nyirenda, S.P., Sileshi, G., Belmain, S.R., Kamanula, J.F., Mvumi, B., Sola, P., Nyirenda, G.K.C., Stevenson, P.C., 2011. Farmers' ethno-ecological knowledge of vegetable pests and their management using pesticidal plants in Northern Malawi and Eastern Zambia. Afr. J. Agric. Res. 6, 1525–1537.
Sarasan, V., Kite, G.C., Sileshi, G., Stevenson, P.C., 2011. Applications of phytochemical and in vitro techniques for reducing over-harvesting of medicinal and pesticidal plants and generating income for the rural poor. Plant Cell Rep. 30, 1163–1172.
Schrire, B.D., 2005. Tribe Millettieae. In: Lewis, G., Schrire, B., Mackinder, B., Lock, M. (Eds.), Legumes of the World. Royal Botanic Gardens, Kew, pp. 367–387 (*Tephrosia* on p. 386).
Sileshi, G., Mafongoya, P.L., Kwesiga, F., Nkunika, P., 2005. Termite damage to maize grown in agroforestry systems, traditional fallows and monoculture on nitrogen-limited soils in eastern Zambia. Agric. For. Entomol. 7, 61–69.
Sirrine, D., Shennan, C., Sirrine, J.R., 2010. Comparing agroforestry systems' ex ante adoption potential and ex post adoption: on-farm participatory research from southern Malawi. Agroforestry Syst. 79, 253–266.
Slade, D., Ferreira, D., Marais, J.P.J., 2005. Circular dichroism, a powerful tool for the assessment of absolute configuration of flavonoids. Phytochemistry 66, 2177–2215.
Sun, Y., Skinner, D.Z., Liang, G.H., Hulbert, S.H., 1994. Phylogenetic analysis of sorghum and related taxa using internal transcribed spacers of nuclear ribosomal DNA. Theor. Appl. Genet. 89, 26–32.
Swofford, D.L., 2002. Phylogenetic Analysis Using Parsimony (∗ and other methods), 4.0b10. Sinaur Associates, Sunderland, Massachusetts.
Taberlet, P., Gielly, L., Pautou, G., Bouvet, J., 1991. Universal primers for amplification of 3 noncoding regions of chloroplast DNA. Plant Mol. Biol. 17, 1105–1109.
Veitch, N.C., Regos, I., Kite, G.C., Treutter, D., 2011. Acylated flavonol glycosides from the forage legume, *Onobrychis viciifolia* (sainfoin). Phytochemistry 72, 423–429.
Vleggaar, R., Smalberg, T.M., Dewaal, H.L., 1973. Flavonoids from *Tephrosia* 5. Structure of tephrostachin. J. South Afr. Chem. Inst. 26, 71–73.
Wangensteen, H., Alamgir, M., Rajia, S., Samuelsen, A.B., Malterud, K.E., 2005. Rotenoids and isoflavones from *Sarcolobus globosus*. Planta Med. 71, 754–758.
Wu, T.-S., 1989. Flavonoids from root bark of *Citrus sinensis* and *C. nobilis*. Phytochemistry 28, 3558–3560.
Ye, H., Chen, L., Li, Y., Peng, A., Fu, A., Song, H., Tang, M., Luo, H., Luo, Y., Xu, Y., Shi, J., Wei, Y., 2008. Preparative isolation and purification of three rotenoids and one isoflavone from the seeds of *Millettia pachycarpa* Benth. by high-speed counter-current chromatography. J. Chromatogr. A 1178, 101–107.